Co-Design Strategies for AFSIW-Based Remote Antenna Units for RFoF

Olivier Caytan*, Igor Lima de Paula*, Laurens Bogaert†, Joris Van Kerrebrouck*,
Arno Moerman*, Mohammad Muneeb†, Guy Torfs*, Johan Bauwelinck*,
Piet Demeester*, Günther Roelkens†, Sam Lemey*, Hendrik Rogier*
*IDLab, Dept. of Information Technology, Ghent University/imec, Ghent, Belgium (Olivier.Caytan@UGent.be)
†Photonics Research Group, Dept. of Information Technology, Ghent University/imec, Ghent, Belgium

***Abstract*—This contribution discusses several recently proposed remote antenna units (RAUs) based on air-filled substrate-integrated-waveguide technology, specifically focusing on the co-design between antenna elements and optoelectronic transducers. These include two passive sub-6 GHz transmit RAUs and one active mmWave transmit RAU. It is concluded that the RAU's performance benefits from a thorough co-design, aiming for a conjugate-match between both components, when compared to a diakoptic design procedure, optimizing both components separately. Specifically, this approach resulted in a significant miniaturization of the sub-6 GHz RAU, while in case of the mmWave RAU, the efficiency was improved.**

***Index Terms*—Air-filled substrate-integrated-waveguide, radio-over-fiber, antenna arrays, co-design, distributed antenna systems**

I. Introduction

Fifth-generation (5G) cellular networks remain under active development. In the meantime, research towards beyond-5G networks is already in full swing, aspiring trade-offs between latency, throughput and reliability surpassing those of 5G, to enable exciting new applications including holographic telepresence, multisensory augmented/virtual reality (AR/VR) [1], and connected robotics and autonomous systems (CRAS) [2]. It is expected that these bold ambitions will be fulfilled, not only by relying on disruptive technologies such as intelligent reflective surfaces (IRSs) [3] and/or large intelligent surfaces (LISs) [4], but also by continuing existing trends [2], such as exploiting fresh frequency spectrum at mmWave and even THz frequencies, cell size reduction, and deploying massive multi-antenna systems to enhance capacity and reliability through multiple-in multiple-out (MIMO) techniques. Combined with larger bandwidth operation at sub-6 GHz and mmWave frequencies, the efficient routing of the RF signals to the massive number of antennas puts designers before huge challenges.

Microwave photonics, and more in particular, RF-over-fiber (RFoF) techniques [5] provide an interesting solution to the problem. RFoF architectures exploit the attractive properties of optical fiber, being low loss, high bandwidth and immunity to electromagnetic interference, for the efficient exchange of broadband RF signals between a central office (CO) and several remote antenna units (RAUs). Specifically, the RF signals are immediately modulated on the optical carrier, which leads to power-efficient RAUs with a minimal number of components, only including optoelectronic transducers, electrical amplifiers and antennas, while avoiding power-hungry mixers. As a result, the CO centralizes synchronized control over the wireless signals and allows to share expensive equipment between RAUs, making it a powerful and highly cost-effective solution [6]. Since it is not necessary that RAUs form a co-located array, RFoF architectures are also ideally suited for implementing distributed antenna systems (DASs). Indeed, RFoF-based DASs have proven to be a key technology to unlock high-throughput high-reliability mmWave coverage by minimizing the occurrence of line-of-sight (LoS) blockage and countering the more adverse propagation properties of mmWaves [7]. It can be concluded that development of cost-effective and high-performance multi-antenna systems at sub-6 GHz and mmWave frequencies deserves serious research effort.

Recently, antenna systems implemented in air-filled substrate-integrated waveguide (AFSIW) technology [8] have been identified as ideal candidates for realizing highly integrated and efficient RAUs [9]. Essentially, AFSIW technology enables compact, planar implementation of conventional air-filled rectangular waveguides. By first creating an air-filled cavity within the substrate of a multi-layer PCB [10], [11], a 3D printed substrate [12], or even within a silicon wafer through micromachining [13], [14], and subsequently metalizing its newly created inner sidewalls, a variety of compact and highly efficient mmWave components can be implemented, including antennas [11], [13]. Since the air-filled cavity contains the component's electromagnetic fields, and the metalization prevents the fields from penetrating in the substrate material, the resulting AFSIW-based antenna elements (AEs) are highly efficient, exhibit excellent antenna/platform isolation, and allow for array deployment with limited mutual coupling [11]. Nevertheless, compatibility with the employed planar technology is retained, guaranteeing compact integration of AFSIW-based AEs with active (opto)electronics.

This contribution discusses several highly integrated and power-efficient transmit RAUs based on AFSIW technology, with a particular focus on the applied co-design strategy. First, two passive sub-6 GHz designs [15], [16] are described, which maximize power transfer from the optical to the electrical domain through dedicated impedance matching. Next, the attention shifts towards an active mmWave RAU [17] that incorporates a 1×4 uniform linear array (ULA), an optoelec-

tronic receiver chain with electrical amplification per AE, and an in-house developed optical beamforming network (OBFN).

This paper is organized as follows. Section II discusses the co-design strategy of the two passive sub-6 GHz RAUs, while Section III focuses on the active mmWave design incorporating optical beamforming. A conclusion is formulated in Section IV.

II. Sub-6 GHz Passive Transmit RAUs

Both sub-6 GHz transmit RAUs [15], [16] are intended for application in an RFoF scheme and have been developed within the framework of the beyond-5G ATTO system [18]. Its target application is a futuristic factory, populated by a vast amount of autonomous robots, each requiring time-critical operation, and reliable high-throughput connectivity to remote computing resources. This results in a challenging trade-off between throughput, reliability, latency and user-density, well out of reach of 5G systems. As a solution, [18] proposes an ultra-dense cellular system with an RFoF interconnection scheme as backbone. To make this solution technically and economically viable, the development of ultra-low power and cost-effective RAUs is required. To this end, both designs [15], [16] adopt strict design constraints, most importantly omitting all active electronics. In the downlink, this enforces a passive conversion from optical to electrical domain, requiring the RF signal intended for wireless transmission to be extracted entirely from the illuminated photodiode without amplification, severely limiting the radiated RF power. Nevertheless, both designs carefully optimize the impedance matching between antenna and photodiode within the operational bandwidth, significantly enhancing the radiated power to a level acceptable for a system involving very short propagation distances, such as in [18]. Both designs [15], [16] leverage a compact and highly efficient AFSIW antenna as a platform on which only a photodiode and impedance matching network (IMN) are integrated, further maximizing power efficiency.

The resulting transmit RAUs are compact, energy-efficient, cost-effective and exhibit very low complexity, consisting only of a photodiode, a bias tee to apply a DC bias voltage to the photodiode, a passive IMN and an AE. The next subsections examine each unit's co-design procedure in more detail.

A. Design I: Diakoptic Approach

The first passive RAU [15] targets the frequency band ranging from 3.3 GHz to 3.7 GHz. A diakoptic design procedure has been adopted, which involves separate optimization of the AFSIW AE and the IMN/photodiode combination. The AFSIW antenna is matched to a $50\,\Omega$ reference impedance within the considered frequency band by optimizing its dimensions, while the IMN is optimized for maximum power transfer from the photodiode's output impedance to an ideal $50\,\Omega$ antenna. This approach, facilitated by the high antenna/platform isolation offered by AFSIW-based antenna topologies, slightly simplifies the design process, but more importantly, it also allows convenient characterization of the separate subsystems. As an evident downside, designing both subsystems separately with respect to a fixed resistive reference impedance potentially leads to a sub-optimal unit.

The RAU, presented schematically in Fig. 1a, is based on a highly efficient AFSIW cavity-backed slot antenna [10]. It is composed of four single-layer PCBs. The first PCB, based on a $0.508\,\mathrm{mm}$-thick RO4350B high-frequency laminate and referred to as the O/E PCB, integrates the bias tee's choke inductor, the IMN, and the photodiode, on which a multimode fiber pigtail is attached with index-matching epoxy. The rectangular air-filled region containing the antenna's fields is created by milling of the two central $1.55\,\mathrm{mm}$-thick FR-4 cavity PCBs and subsequent metalization of the created inner edges. The metalization is key in maintaining the antenna's high radiation efficiency, since it prevents the fields from penetrating the lossy FR-4. The air-filled region is enclosed by the ground plane of the O/E PCB and the inner metallic layer of the slot PCB (also based on $0.508\,\mathrm{mm}$-thick RO4350B). A radiating rectangular slot is created in the slot PCB's inner metallic layer, as shown in Fig. 1a. In fact, the slot divides the air-filled cavity into two coupled half-mode cavities. As such, the structure supports two distinct resonances which, in combination with the air substrate, significantly increase the antenna's impedance bandwidth ($\geq$ 10 dB return loss w.r.t. $50\,\Omega$ from 3.1 to 3.9 GHz). One of these half-mode AFSIW cavities is excited by a probe connected to the O/E PCB's circuitry. The probe is AC coupled to the antenna, preventing that the AFSIW cavity imposes a zero-bias on the photodetector.

As described in [15], a lossless third-order band-pass Chebyshev IMN is synthesized based on the measured output impedance of the photodiode, which is approximated accurately by a resistor/capacitor series combination. The IMN maximizes the minimum transducer gain (defined using the photodiode as the generator and the $50\,\Omega$ antenna as the load) within the frequency band of interest. After applying several transformations on the ideal IMN in order to facilitate a practical implementation, the model shown in Fig. 1b is obtained. It consists of the equivalent circuit of the photodiode, the IMN (partly lumped, partly distributed), and the ideal $50\,\Omega$ antenna. The practical implementation of the nearly lossless IMN is shown in Fig. 1a. A lumped chip inductor, a tunable inductor based on a shorted grounded coplanar waveguide (GCPW) section and the photodiode's wire bonds all contribute to the IMN's series inductance of 15.3 nH. Furthermore, the open half-wavelength shunt stubs are realized by radial stubs.

A full-wave/circuit co-simulation model of the RAU was optimized in CST Microwave Studio, yielding a $-3\,\mathrm{dB}$ gain bandwidth ranging from 3.25 GHz to 3.74 GHz and an average transducer gain of $60.9\,\%$ in the frequency band of interest. The design procedure was thoroughly validated by measurements on a prototype, conforming the performance observed in simulation, as described in [15]. The simulated and measured values of several key performance metrics are compared in Table I.

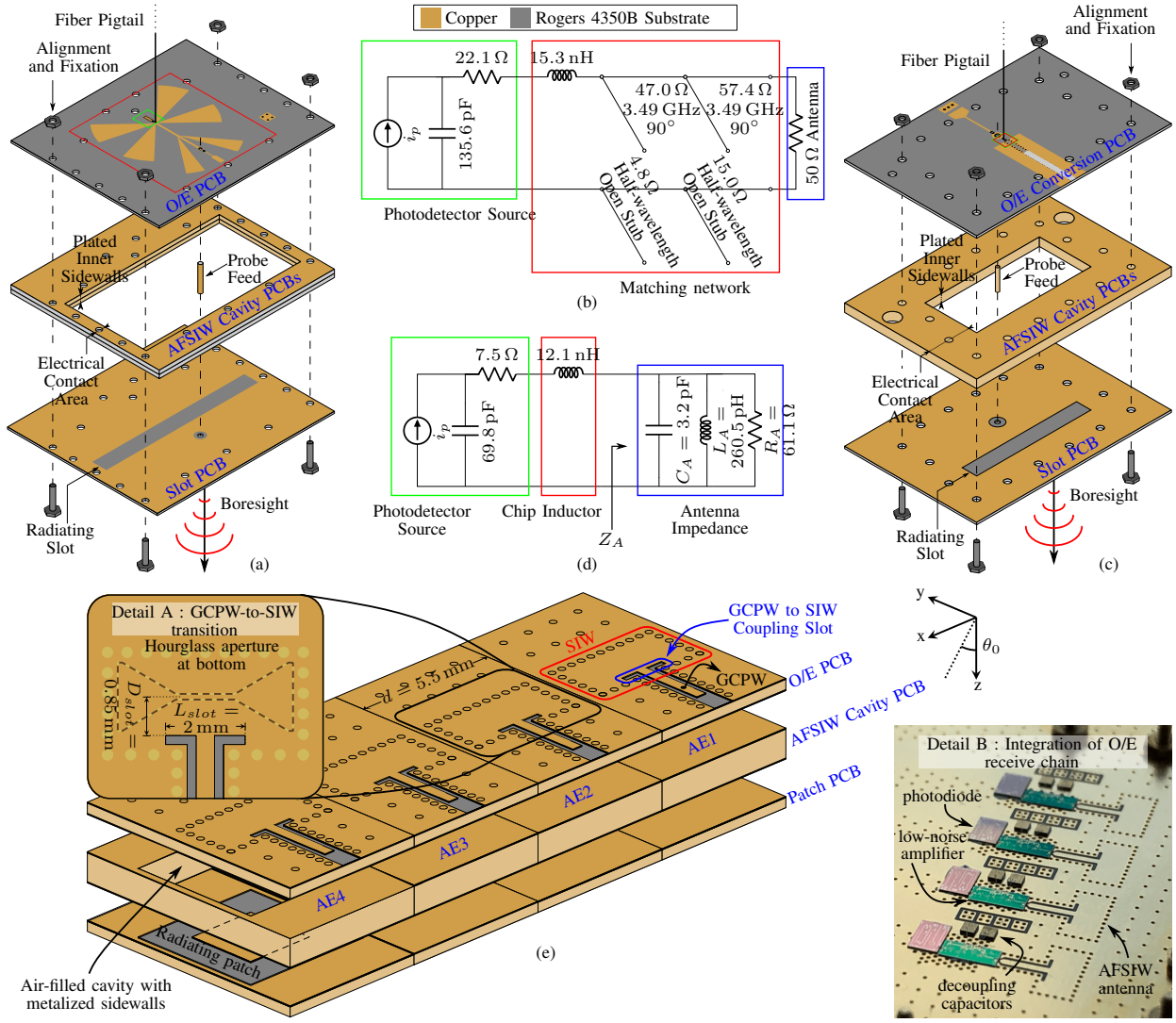

Fig. 1. (a) Exploded view and (b) principle of operation of the sub-6 GHz passive remote antenna unit (RAU) with lumped/distributed impedance matching network (Design I) [15], (c+d) the conjugate-matched sub-6 GHz passive RAU (Design II) [16], and (e) the active mmWave RAU, consisting of four antenna elements (AE1–AE4) [17].

TABLE I
SUB-6 GHz PASSIVE TRANSMIT REMOTE ANTENNA UNITS: MEASURED (SIMULATED) PERFORMANCE.

Design	**Footprint** [$\lambda \times \lambda$]	**Gain [dBi]** (normalized w.r.t SE [16])	-3 dB **Gain Bandwidth [GHz]**	**E/H-Plane HPBW** [°]
I: Diakoptic	1.19×0.66	10.8 (10.2)	3.27–3.75 (3.25–3.74)	150/55 (105/56)
II: Conjugate Matched	0.84×0.41	10.5 (10.3)	4.98–6.00 (5.07–5.91)	117/62 (102/68)

B. Design II: Conjugate-Matched Approach

The second passive sub-6 GHz RAU [16] targets the 5.15–5.85 GHz frequency band. Although the first design is a highly integrated unit, the diakoptic design procedure might still lead to a unit with sub-optimal performance. Therefore, a more intricate co-design is conducted for the second design, where the common reference impedance is relinquished and a conjugate match between the AFSIW antenna and photodiode is pursued, instead. This results in a considerably more compact RAU (Fig. 1c) where the area-consuming distributed elements and their associated loss and spurious radiation are eliminated. In addition, the antenna is also miniaturized significantly.

Similar to the first design, the procedure starts by synthesizing an ideal lossless second-order band-pass Chebyshev IMN based on the measured output impedance of the photodiode, resulting in the circuit model in Fig. 1d. The diakoptic approach of Design I would realize the resonant shunt LC ($L_A||C_A$) tank as a large distributed element and identify the resistance R_A with the matched AE in combination with a quarter-wave transformer. Two coupled half-mode AFSIW

cavities were required to obtain adequate impedance matching to the $50\,\Omega$ reference impedance over the relatively wide frequency band of interest. Instead, here, the impedance Z_A of the entire shunt RLC tank ($R_A||L_A||C_A$) is identified with the impedance of a single cavity resonator with a very low quality factor of 6.8, which can be practically realized by means of only one radiating half-mode AFSIW cavity. Finally, the series inductance of $12.1\,\mathrm{nH}$, being the only remaining part of the IMN, is realized similarly as Design I.

After full-wave/circuit co-optimization, a $-3\,\mathrm{dB}$ gain bandwidth ranging from $5.07\,\mathrm{GHz}$ to $5.91\,\mathrm{GHz}$ and an average transducer gain of $19.2\,\%$ in the frequency band of interest are predicted. Measurements confirm the high performance observed during simulation (see Table I), validating the followed design procedure. A significant area reduction is obtained with respect to the first design. It should be noted that, when comparing Designs I and II in terms of obtained transducer gain, the different photodiode impedances must be taken into account.

III. mmWave Active Transmit RAU with Optical Beamforming

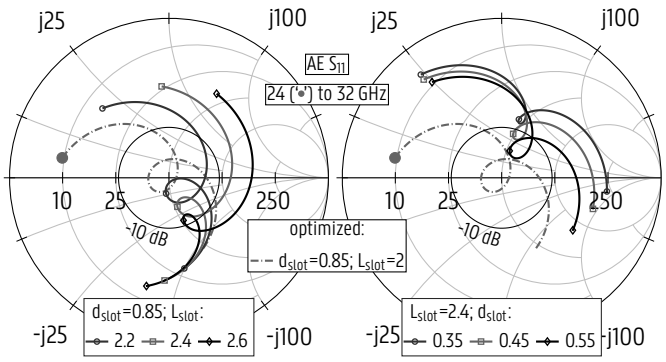

Fig. 2. Parametric analysis of (a) L_{slot} and (b) d_{slot} (see Fig. 1e) for the reflection coefficient of the mmWave AFSIW antenna [17]. The topology's impedance matching flexibility allows to pursue an improved conjugate-match to a variety of source impedances. Specifically, the mmWave RAU's performance can be enhanced, especially for larger scan angles, by reducing the antenna elements' active reflection coefficient (w.r.t. the LNA's output impedance) to below $-9.3\,\mathrm{dB}$ and by increasing the total efficiency to at least $85\,\%$ for scan angles between $\theta_0 = \pm 50^\circ$ in the 26.5–29.5 GHz 5G band.

The attention now shifts towards the mmWave active transmit RAU [17], which is designed for wide-angle beam steering in the 26.5–29.5 GHz n257 5G band, and is ideally suited for application in the mmWave DAS proposed in [7]. mmWave frequencies experience significantly more adverse propagation conditions [7], such as higher path loss, increased outdoor-to-indoor penetration loss, and much more pronounced shadowing. Fortunately, facilitated by the shorter wavelengths, array deployment of a high number of mmWave AEs allows to compensate the increased path losses and to account for user mobility using beam steering. In addition, DASs based on mmWave-over-Fiber RAUs [7] have shown great potential in unlocking reliable indoor high-throughput mmWave coverage by preventing shadowing and LoS blockage.

The mmWave active transmit RAU [17], presented schematically in Fig. 1e, integrates a 1×4 ULA with a dedicated mmWave-over-Fiber receiver for each AE. The 1×4 RAU is complemented by an in-house developed true-time-delay (TTD) OBFN on a photonic integrated circuit (PIC).

The ULA is based on compact cavity-backed patch elements implemented in AFSIW technology, guaranteeing efficient antenna operation and low inter-element coupling. The AFSIW array is also leveraged as a platform to integrate the active (opto)electronics with minimal interconnection losses, maximizing performance. The entire structure is composed of three single-layer PCBs (see Fig. 1e). The central AFSIW Cavity PCB (based on $1\,\mathrm{mm}$-thick FR-4) contains the air-filled cavities of the four antennas, which are created by milling and subsequent edge-plating. For each AE, the O/E PCB (based on $0.254\,\mathrm{mm}$-thick RO4350B) integrates a dedicated photoreceiver chain with a compact feed structure, which efficiently couples the photoreceiver's output power into the air-filled cavity of the corresponding antenna. The feed structures are designed for wideband and efficient operation with minimal back-radiation. They consist of a short GCPW section in combination with a GCPW-to-SIW transition and an hourglass shaped coupling slot in the ground plane [17] (see detail A of Fig. 1e). The third PCB integrates the four radiating patches.

Each mmWave-over-Fiber photoreceiver chain consists of a silicon waveguide coupled Ge-on-Si photodiode, a GaAs low-noise amplifier (LNA) and decoupling chip capacitors. The LNA exhibits a noise figure of only $2.1\,\mathrm{dB}$ and covers a 23.5–31.5 GHz 3 dB gain bandwidth with a maximum gain of $24\,\mathrm{dB}$ [19]. Its output is designed to be matched to $50\,\Omega$, although the output impedance is slightly frequency-dependent.

The OBFN PIC [17] is separately packaged and implemented on imec's passive silicon photonics platform. Its four integrated switchable optical delay lines offer a maximum delay of $49.6\,\mathrm{ps}$ with 5-bit discrete resolution, supporting TTD beam steering over the array's full grating-lobe-free scan range ($\theta_0 = \pm 50^\circ$), perfectly complementing the RAU.

As annotated in Fig. 1e, the AE spacing d amounts to $5.5\,\mathrm{mm}$ ($0.54\lambda_u$, λ_u being the free-space wavelength at $29.5\,\mathrm{GHz}$), which is selected as a compromise. On the one hand, this ensures a spacing that is tight enough to support a grating-lobe-free scan range of at least $\theta_0 = \pm 50^\circ$. On the other hand, it maintains sufficient inter-element isolation such that the AEs' active reflection coefficients remain sufficiently matched within this scan range in the entire frequency band of interest. Since the LNA's output impedance is matched to $50\,\Omega$, [17] has followed a diakoptic approach, optimizing the array elements' active impedance to match $50\,\Omega$. With this approach, the active reflection coefficient (w.r.t. the LNA's output impedance) of the AEs remains below $-6.5\,\mathrm{dB}$, indicating that at least $78\,\%$ of the LNA's output power is accepted for all considered frequencies and scan angles (up to $\theta_0 = \pm 50^\circ$). An extensive measurement campaign was conducted with a prototype of the fully integrated mmWave transmit RAU, validating the described diakoptic design procedure.

Nevertheless, an improved conjugate-match can be pursued between ULA and LNA by exploiting the impedance matching flexibility offered by the antenna's feed structure [17], which is demonstrated in Fig. 2, showing the influence of the dimensional parameters L_{slot} (Fig. 2a) and d_{slot} (Fig. 2b) on the AEs' input impedance. By means of this more intricate co-design procedure, the active reflection coefficient (w.r.t. the LNA's output impedance) of the AEs can be further reduced to below $-9.3\,\mathrm{dB}$, increasing the minimum fraction of accepted LNA output power to $88\,\%$. In addition, since the improvement is most pronounced for the larger scan angles, this optimization also improves the total efficiency to at least $85\,\%$ for scan angles between $\theta_0 = \pm 50°$. Finally, a future design could benefit from the AEs' impedance matching flexibility by (partly) eliminating the LNA's output impedance matching network and its associated losses, enhancing the proposed mmWave RAU's performance more significantly.

IV. Conclusion

The practical realization of multi-antenna systems, widely considered to be a key technology for 5G and beyond, is greatly facilitated by RF-over-fiber techniques, which exploit optical fiber for the efficient and synchronized exchange of RF signals with remote antenna units (RAUs), making highly innovative antenna systems, such as [7], feasible. Therefore, the development of cost-effective and high-performance RAUs is crucial. Antenna topologies based on air-filled substrate-integrated-waveguide (AFSIW) have been identified as particularly interesting candidates for realizing efficient RAUs [9], with their high antenna/platform isolation facilitating compact integration of the optoelectronic transducers.

In this contribution, we discussed several recently proposed AFSIW-based RAUs, focusing specifically on the co-design between antenna elements and optoelectronic transducers. These include two passive sub-6 GHz transmit RAUs and one active mmWave transmit RAU, incorporating beam forming. It is concluded that the RAU's performance benefits from a thorough co-design, aiming for a conjugate-match between both components, when compared to a diakoptic design procedure, optimizing both components separately. Specifically, this approach resulted in a significant miniaturization of the sub-6 GHz RAU, while in case of the mmWave RAU, the efficiency was improved.

Acknowledgment

This research was supported by Ghent University (Methusalem projects "Smart Photonic Chips" and "SHAPE") and by the ERC (Grant ATTO (695495)).

References

[1] M. Giordani, M. Polese, M. Mezzavilla, S. Rangan, and M. Zorzi, "Toward 6G Networks: Use Cases and Technologies," *IEEE Commun. Mag.*, vol. 58, pp. 55–61, March 2020.

[2] W. Saad, M. Bennis, and M. Chen, "A Vision of 6G Wireless Systems: Applications, Trends, Technologies, and Open Research Problems," *IEEE Netw.*, vol. 34, no. 3, pp. 134–142, 2020.

[3] Q. Wu and R. Zhang, "Towards Smart and Reconfigurable Environment: Intelligent Reflecting Surface Aided Wireless Network," *IEEE Commun. Mag.*, vol. 58, pp. 106–112, January 2020.

[4] S. Hu, F. Rusek, and O. Edfors, "Beyond Massive MIMO: The Potential of Data Transmission With Large Intelligent Surfaces," *IEEE Trans. Signal Process.*, vol. 66, pp. 2746–2758, May 2018.

[5] D. Novak, R. B. Waterhouse, A. Nirmalathas, C. Lim, P. A. Gamage, T. R. Clark, M. L. Dennis, and J. A. Nanzer, "Radio-Over-Fiber Technologies for Emerging Wireless Systems," *IEEE J. Quantum Electron.*, vol. 52, no. 1, pp. 1–11, 2016.

[6] V. A. Thomas, M. El-Hajjar, and L. Hanzo, "Performance Improvement and Cost Reduction Techniques for Radio Over Fiber Communications," *IEEE Commun. Surv. & Tutorials*, vol. 17, no. 2, pp. 627–670, 2015.

[7] A. Moerman, J. Van Kerrebrouck, O. Caytan, I. Lima de Paula, L. Bogaert, G. Torfs, P. Demeester, H. Rogier, and S. Lemey, "Beyond 5G Without Obstacles: mmWave-over-Fiber Distributed Antenna Systems," *IEEE Commun. Mag.*, vol. 60, pp. 27–33, January 2022.

[8] A. Belenguer, H. Esteban, and V. E. Boria, "Novel Empty Substrate Integrated Waveguide for High-Performance Microwave Integrated Circuits," *IEEE Trans. Microw. Theory Techn.*, vol. 62, pp. 832–839, April 2014.

[9] S. Lemey, O. Caytan, Q. Van den Brande, I. L. d. Paula, L. Bogaert, H. Li, J. V. Kerrebrouck, A. C. F. Reniers, B. Smolders, J. Bauwelinck, P. Demeester, G. Torfs, D. V. Ginste, S. Verstuyft, B. Kuyken, and H. Rogier, "Air-filled Substrate-Integrated Waveguide Technology for Broadband and Highly-Efficient Photonic-Enabled Antenna Systems," in *2020 XXXIIIrd General Assembly and Scientific Symposium of the International Union of Radio Science*, pp. 1–4, 2020.

[10] Q. Van den Brande, S. Lemey, J. Vanfleteren, and H. Rogier, "Highly Efficient Impulse-Radio Ultra-Wideband Cavity-Backed Slot Antenna in Stacked Air-Filled Substrate Integrated Waveguide Technology," *IEEE Trans. Antennas Propag.*, vol. 66, no. 5, pp. 2199–2209, 2018.

[11] I. Lima de Paula, S. Lemey, D. Bosman, Q. Van den Brande, O. Caytan, J. Lambrecht, M. Cauwe, G. Torfs, and H. Rogier, "Cost-Effective High-Performance Air-Filled SIW Antenna Array for the Global 5G 26 GHz and 28 GHz Bands," *IEEE Antennas Wirel. Propag. Lett.*, vol. 20, no. 2, pp. 194–198, 2021.

[12] K. Yavuz Kapusuz, S. Lemey, P. Demeester, and H. Rogier, "Additive-Manufacturing-Enabled Air-Filled Substrate Integrated Waveguide Microwave Components," in *2018 IEEE International Symposium on Antennas and Propagation & USNC/URSI National Radio Science Meeting*, pp. 939–940, 2018.

[13] Q. Van den Brande, S. Lemey, S. Cuyvers, S. Poelman, L. De Brabander, O. Caytan, L. Bogaert, I. L. D. Paula, S. Verstuyft, A. C. F. Reniers, B. Smolders, B. Kuyken, D. V. Ginste, and H. Rogier, "A Hybrid Integration Strategy for Compact, Broadband, and Highly Efficient Millimeter-Wave On-Chip Antennas," *IEEE Antennas Wirel. Propag. Lett.*, vol. 18, no. 11, pp. 2424–2428, 2019.

[14] B. Beuerle, J. Campion, U. Shah, and J. Oberhammer, "A Very Low Loss 220–325 GHz Silicon Micromachined Waveguide Technology," *IEEE Trans. Terahertz Sci. Technol.*, vol. 8, no. 2, pp. 248–250, 2018.

[15] O. Caytan, L. Bogaert, H. Li, J. Van Kerrebrouck, S. Lemey, G. Torfs, J. Bauwelinck, P. Demeester, S. Agneessens, D. V. Ginste, and H. Rogier, "Passive Opto-Antenna as Downlink Remote Antenna Unit for Radio Frequency Over Fiber," *J. Lightw. Technol.*, vol. 36, no. 19, pp. 4445–4459, 2018.

[16] O. Caytan, L. Bogaert, H. Li, J. V. Kerrebrouck, S. Lemey, S. Agneessens, J. Bauwelinck, P. Demeester, G. Torfs, D. V. Ginste, and H. Rogier, "Compact and wideband transmit opto-antenna for radio frequency over fiber," *Opt. Express*, vol. 27, pp. 8395–8413, Mar 2019.

[17] I. Lima de Paula, L. Bogaert, O. Caytan, J. Van Kerrebrouck, A. Moerman, M. Muneeb, Q. Van den Brande, G. Torfs, J. Bauwelinck, H. Rogier, P. Demeester, G. Roelkens, S. Lemey, and S. Lemey, "Air-Filled SIW Remote Antenna Unit with True Time Delay Optical Beamforming for mmWave-over-Fiber Systems," *J. Lightw. Technol.*, pp. 1–15, 2022.

[18] G. Torfs, H. Li, S. Agneessens, J. Bauwelinck, L. Breyne, O. Caytan, W. Joseph, S. Lemey, H. Rogier, A. Thielens, D. Vande Ginste, J. V. Kerrebrouck, G. Vermeeren, X. Yin, and P. Demeester, "ATTO: Wireless Networking at Fiber Speed," *J. Lightw. Technol.*, vol. 36, no. 8, pp. 1468–1477, 2018.

[19] L. Bogaert, H. Li, K. Van Gasse, J. Van Kerrebrouck, J. Bauwelinck, G. Roelkens, and G. Torfs, "36 Gb/s Narrowband Photoreceiver for mmWave Analog Radio-Over-Fiber," *J. Lightw. Technol.*, vol. 38, no. 12, pp. 3289–3295, 2020.